

Deconvolving Images with Unknown Boundaries Using the Alternating Direction Method of Multipliers

Mariana S. C. Almeida and Mário A. T. Figueiredo, *Fellow, IEEE*

Abstract—The *alternating direction method of multipliers* (ADMM) has sparked recent interest as an efficient optimization tool for solving imaging inverse problems, such as deconvolution and reconstruction. ADMM-based approaches achieve state-of-the-art speed, by adopting a *divide and conquer* strategy that splits a hard problem into simpler, efficiently solvable sub-problems (e.g., using fast Fourier or wavelet transforms, or proximity operators with low computational cost). In deconvolution problems, one of these sub-problems involves a matrix inversion (i.e., solving a linear system), which can be performed efficiently (in the discrete Fourier domain) if the observation operator is circulant, that is, under periodic boundary conditions. This paper proposes an ADMM approach for image deconvolution in the more realistic scenario of unknown boundary conditions. To estimate the image and its unknown boundary, we model the observation operator as a composition of a cyclic convolution with a spatial mask that excludes those pixels where the cyclic convolution is invalid, i.e., the unknown boundary. The proposed method can also handle, at no additional cost, problems that combine inpainting (recovery of missing pixels) and deblurring. We show that the resulting algorithm inherits the convergence guarantees of ADMM and illustrate its state-of-the-art performance on non-cyclic deblurring (with and without inpainting of interior pixels) under total-variation (TV) regularization.

Index Terms—Image deconvolution, image deblurring, alternating direction method of multipliers (ADMM), variable splitting, non-cyclic deconvolution, inpainting, total variation.

I. INTRODUCTION

The *alternating direction method of multipliers* (ADMM), originally proposed in the 1970's [15], emerged recently as a highly flexible and efficient tool for addressing several imaging inverse problems, such as denoising [22], [14], deblurring [2], inpainting [2], reconstruction [18], motion segmentation [26], to mention only a few classical problems. ADMM-based approaches make use of variable splitting, thus allowing a straightforward treatment of various prior/regularization terms [1], such as those based on frame representations and on the well known *total-variation* (TV) norm [20], as well as the seamless inclusion of several types of constraints, such as positivity [22], [14]. ADMM is equivalent or closely related to other techniques, namely the so-called *Bregman* and *split Bregman* methods [16], [6], [25] and the *Douglas-Rachford splitting* [5], [9], [12], [13]. For a recent review of ADMM and its many applications, as well as a comprehensive literature review, see [5].

Most ADMM-based algorithms for imaging inverse problems involve, as one of their steps, the solution of a linear system (equivalently, a large matrix inversion) [2], [6], [14],

[23]. This fact is simultaneously a blessing and a curse: on the one hand, the matrix being inverted is related to the Hessian of the underlying objective function, thus providing the algorithms with second order information and, arguably, justifying the excellent speed of these methods; on the other hand, this inversion (due to its typically huge size) limits their applicability to problems where it can be efficiently computed. For ADMM-based image deconvolution algorithms [2], [6], [14], [23], this inversion can be efficiently computed using the *fast Fourier transform* (FFT), as long as the convolution operator is cyclic/periodic (or assumed to be so), thus diagonal in the discrete Fourier domain. However, in most real problems, the convolution is not cyclic, thus the required matrix inversion can not be solved efficiently using the FFT.

In an image deconvolution problem, the pixels located near the boundary of the observed image depend on pixels that lie outside of its domain; accordingly, it is necessary to make some assumptions about the values of those unobserved pixels, i.e., to adopt some *boundary condition*. The usual approach is to assume one of the classical boundary conditions imported from the partial differential equations literature, namely: periodic boundary condition; Dirichlet boundary condition, where the external boundary pixels are zero-valued; Neumann (or reflexive) boundary condition, where the external boundary is a reflection of interior region next to it; anti-reflexive boundary condition, where the external boundary is the negative of what it is in the Neumann case [8], [11]. As illustrated in Figure 1, all these standard boundary conditions are quite artificial and do not correspond to realistic imaging systems; they are merely motivated by computational convenience considerations.

Assuming a periodic boundary condition has the advantage of allowing a very fast implementation of the convolution as a point-wise multiplication in the *discrete Fourier transform* (DFT) domain, with both the direct and inverse DFT being very efficiently implemented by the FFT. However, in real problems, there is no reason for the external (unobserved) pixels to follow periodic (or any other) boundary conditions. A well known consequence of this mismatch is a degradation of the deconvolved images, namely the appearance of ringing artifacts emanating from the boundaries (see Figs. 2 (a) and 3 (a)). These artifacts can be reduced by pre-processing the image to reduce the spurious discontinuities at the image boundaries created by the periodicity assumption; this is what is done by the well-known “edgetaper” function in the *MATLAB Image Processing Toolbox*. In a more sophisticated version of this idea that was recently proposed, the observed image is extrapolated to create a larger image with smooth boundary conditions [17].

Convolution under Dirichlet boundary conditions can still



Fig. 1. Illustration of the assumptions underlying the periodic, Neumann, and Dirichlet boundary conditions.

be carried out in the DFT domain, using the classical zero-padding technique and embedding the non-periodic convolution into a larger periodic one. However, in addition to the mismatch problem pointed out in the previous paragraph (there is usually no reason to assume that the boundary pixels are zero), this choice has another drawback: in the context of ADMM-based methods, the zero-padding technique does not allow the required matrix inversion (mentioned above) to be efficiently computed by resorting to the FFT [4].

A. Contributions

Instead of choosing a specific boundary condition or applying a boundary smoothing strategy, a more realistic option is to consider that the external boundary pixels are unknown, which is what actually happens in most imaging systems. This approach can be formulated as a simultaneous deconvolution and inpainting problem, where the unobserved boundary pixels around the image are estimated while the image is simultaneously being deconvolved. Although this formulation has been used before (see [8], [19]), it has not been addressed using state-of-the-art ADMM-based methods. In fact, ADMM is particularly suited to handle this formulation.

The observation model involves the composition of a periodic convolution with a spatial mask; the former corresponds to a point-wise multiplication in the spatial domain, while the later corresponds to a point-wise multiplication in the DFT domain. We will show how, in the context of the ADMM algorithm, these two operations can be decoupled and handled separately.

Very recently, a related approach (although not explicitly described as such) was proposed in [21], by exploiting earlier work for deconvolution without boundary artifacts under quadratic regularization [19]. That approach requires solving, at each iteration, a linear system of the size of the number of unknown pixels, which can only be done numerically. In contrast, every update equation of the ADMM algorithm herein proposed has closed form, and the method is shown to satisfy sufficient conditions for convergence.

The proposed method will be experimentally illustrated using total-variation (TV) deblurring (by adapting the state-of-the-art algorithm described in [23]); the results show the advantage of our approach over the use of the “edgetaper” function (in terms of improvement in SNR) and over an adaptation of the recent strategy of [21] (in terms of speed). Finally, our approach is also tested on inverse problems where the observation model consists of a (non-cyclic) deblurring followed by a generic loss of pixels (inpainting problems). Arguably due to its complexity, this problem has not been often addressed in the literature, although it is a relevant one: consider the problem of deblurring an image in which some pixel values are inaccessible, *e.g.*, because they are saturated, thus should not be taken into account.

B. Outline

The remaining sections of the paper are organized as follows. Section II reviews the ADMM. Section III describes our ADMM-based approach in the context of TV-based image deconvolution. An experimental comparison of our method versus the use of the well known “edgetapper” function and the use of the recent strategy of [21], is reported in Section IV; that section also illustrates the use of the proposed method for simultaneous deblurring and inpainting. Finally, Section V concludes the manuscript.

Notation: we use bold lower case to denote vectors (*e.g.* \mathbf{x} , \mathbf{y} , \mathbf{u}), and bold upper case (Roman or Greek) to denote matrices (*e.g.*, \mathbf{A} , \mathbf{D} , $\mathbf{\Upsilon}$, $\mathbf{\Gamma}$). The superscript T denotes vector/matrix transpose, or conjugate transpose in the case of complex vectors/matrices.

II. THE ALTERNATING DIRECTION METHOD OF MULTIPLIERS (ADMM)

A. The Standard ADMM Algorithm

Consider an unconstrained optimization problem

$$\min_{\mathbf{z} \in \mathbb{R}^n} f(\mathbf{z}) + g(\mathbf{G}\mathbf{z}), \quad (1)$$

where $f : \mathbb{R}^n \rightarrow \bar{\mathbb{R}} = \mathbb{R} \cup \{+\infty\}$ and $g : \mathbb{R}^p \rightarrow \bar{\mathbb{R}}$ are proper, closed, convex functions, and $\mathbf{G} \in \mathbb{R}^{p \times n}$ is a matrix. The ADMM algorithm for this problem (presented in Algorithm 1) can be motivated and derived from different perspectives (*e.g.*,

augmented Lagrangian, Douglas-Rachford splitting); for a recent comprehensive review, see [5]. Convergence of ADMM was shown in [12], where the following theorem was proved.

Theorem 1: Consider problem (1), where $\mathbf{G} \in \mathbb{R}^{p \times n}$ has full column rank and $f : \mathbb{R}^d \rightarrow \mathbb{R}$ and $g : \mathbb{R}^p \rightarrow \mathbb{R}$ are closed, proper, and convex functions. Consider arbitrary $\mu > 0$, $\mathbf{u}_0, \mathbf{d}_0 \in \mathbb{R}^p$. Let $\eta_k \geq 0$ and $\rho_k \geq 0$, for $k = 0, 1, \dots$, be two sequences such that $\sum_{k=0}^{\infty} \eta_k < \infty$ and $\sum_{k=0}^{\infty} \rho_k < \infty$. Consider three sequences $\mathbf{z}_k \in \mathbb{R}^n$, $\mathbf{u}_k \in \mathbb{R}^p$, and $\mathbf{d}_k \in \mathbb{R}^p$, for $k = 0, 1, \dots$, satisfying

$$\begin{aligned} \left\| \mathbf{z}_{k+1} - \arg \min_{\mathbf{z}} f(\mathbf{z}) + \frac{\mu}{2} \|\mathbf{G}\mathbf{z} - \mathbf{u}_k - \mathbf{d}_k\|_2^2 \right\| &\leq \eta_k \\ \left\| \mathbf{u}_{k+1} - \arg \min_{\mathbf{u}} g(\mathbf{u}) + \frac{\mu}{2} \|\mathbf{G}\mathbf{z}_{k+1} - \mathbf{u} - \mathbf{d}_k\|_2^2 \right\| &\leq \rho_k \\ \mathbf{d}_{k+1} &= \mathbf{d}_k - (\mathbf{G}\mathbf{z}_{k+1} - \mathbf{u}_{k+1}). \end{aligned}$$

Then, if (1) has a solution, say \mathbf{z}^* , the sequence $\{\mathbf{z}_k\}$ converges to \mathbf{z}^* . If (1) does not have a solution, then at least one of the sequences $(\mathbf{u}_1, \mathbf{u}_2, \dots)$ or $(\mathbf{d}_1, \mathbf{d}_2, \dots)$ diverges.

Algorithm 1: ADMM

```

1 Initialization: set  $k = 0$ , choose  $\mu > 0$ ,  $\mathbf{u}_0$ , and  $\mathbf{d}_0$ .
2 repeat
3    $\mathbf{z}_{k+1} \leftarrow \arg \min_{\mathbf{z}} f(\mathbf{z}) + \frac{\mu}{2} \|\mathbf{G}\mathbf{z} - \mathbf{u}_k - \mathbf{d}_k\|_2^2$ 
4    $\mathbf{u}_{k+1} \leftarrow \arg \min_{\mathbf{u}} g(\mathbf{u}) + \frac{\mu}{2} \|\mathbf{G}\mathbf{z}_{k+1} - \mathbf{u} - \mathbf{d}_k\|_2^2$ 
5    $\mathbf{d}_{k+1} \leftarrow \mathbf{d}_k - (\mathbf{G}\mathbf{z}_{k+1} - \mathbf{u}_{k+1})$ 
6    $k \leftarrow k + 1$ 
7 until stopping criterion is satisfied
```

Under the conditions of *Theorem 1*, convergence holds for any value of $\mu > 0$; however, the choice of this parameter may strongly affect the convergence speed [5]. It is also possible to replace the scalar μ by a positive diagonal matrix $\Upsilon = \text{diag}(\mu_1, \dots, \mu_p)$, which means replacing the quadratic terms of the form $\mu \|\mathbf{G}\mathbf{z} - \mathbf{u} - \mathbf{d}\|_2^2$ by $(\mathbf{G}\mathbf{z} - \mathbf{u} - \mathbf{d})^T \Upsilon (\mathbf{G}\mathbf{z} - \mathbf{u} - \mathbf{d})$.

B. The ADMM For Two or More Functions

Following the formulation proposed in [3], [14], consider a generalization of (1), with $J \geq 2$ functions,

$$\min_{\mathbf{z} \in \mathbb{R}^n} \sum_{j=1}^J g_j(\mathbf{H}^{(j)}\mathbf{z}), \quad (2)$$

where $g_j : \mathbb{R}^{p_j} \rightarrow \bar{\mathbb{R}}$ are proper, closed, convex functions, and $\mathbf{H}^{(j)} \in \mathbb{R}^{p_j \times n}$ are arbitrary matrices. We map this problem into the form (1) as follows: let $f(\mathbf{z}) = 0$; define matrix \mathbf{G} as

$$\mathbf{G} = \begin{bmatrix} \mathbf{H}^{(1)} \\ \vdots \\ \mathbf{H}^{(J)} \end{bmatrix} \in \mathbb{R}^{p \times n}, \quad (3)$$

where $p = p_1 + \dots + p_J$, and let $f_2 : \mathbb{R}^p \rightarrow \bar{\mathbb{R}}$ be defined as

$$g(\mathbf{u}) = \sum_{j=1}^J g_j(\mathbf{u}^{(j)}), \quad (4)$$

where each $\mathbf{u}^{(j)} \in \mathbb{R}^{p_j}$ is a sub-vector of $\mathbf{u} = [(\mathbf{u}^{(1)})^T, \dots, (\mathbf{u}^{(J)})^T]^T$.

The definitions in the previous paragraph lead to an ADMM for problem (2) with the following two key features.

- Firstly, the fact that $f(\mathbf{z}) = 0$ turns line 3 of Algorithm 1 into an unconstrained quadratic problem. Letting Υ be a positive block diagonal matrix (which associates possibly different parameters μ_j to each function g_j)

$$\Upsilon = \text{diag}(\underbrace{\mu_1, \dots, \mu_1}_{p_1 \text{ elements}}, \dots, \underbrace{\mu_j, \dots, \mu_j}_{p_j \text{ elements}}, \dots, \underbrace{\mu_J, \dots, \mu_J}_{p_J \text{ elements}}), \quad (5)$$

the solution of this quadratic problem is given by (denoting $\zeta = \mathbf{u}_k + \mathbf{d}_k$)

$$\begin{aligned} \arg \min_{\mathbf{z}} (\mathbf{G}\mathbf{z} - \zeta)^T \Upsilon (\mathbf{G}\mathbf{z} - \zeta) &= (\mathbf{G}^T \Upsilon \mathbf{G})^{-1} \mathbf{G}^T \Upsilon \zeta \\ &= \left[\sum_{j=1}^J \mu_j (\mathbf{H}^{(j)})^T \mathbf{H}^{(j)} \right]^{-1} \sum_{j=1}^J \mu_j (\mathbf{H}^{(j)})^T \zeta^{(j)}, \quad (6) \end{aligned}$$

with $\zeta^{(j)} = \mathbf{u}_k^{(j)} + \mathbf{d}_k^{(j)}$, where $\zeta^{(j)}$, $\mathbf{u}_k^{(j)}$, and $\mathbf{d}_k^{(j)}$, for $j = 1, \dots, J$, are the sub-vectors of ζ , \mathbf{u}_k , and \mathbf{d}_k , respectively, corresponding to the partition in (3), and the second equality results from the block structure of matrices \mathbf{G} (in (3)) and Υ (in (5)).

- Secondly, the separable structure of g (as defined in (4)) allows decoupling the minimization in line 4 of Algorithm 1 into J independent minimizations, each of the form

$$\mathbf{u}_{k+1}^{(j)} \leftarrow \arg \min_{\mathbf{v} \in \mathbb{R}^{p_j}} g_j(\mathbf{v}) + \frac{\mu_j}{2} \|\mathbf{v} - \mathbf{s}^{(j)}\|_2^2, \quad (7)$$

for $j = 1, \dots, J$, where $\mathbf{s}^{(j)} = \mathbf{H}^{(j)}\mathbf{z}_{k+1} - \mathbf{d}_k^{(j)}$. This minimization corresponds to the so-called *Moreau proximity operator* of g_j/μ (denoted as prox_{g_j/μ_j}) (see [9], [10] and references therein) applied to $\mathbf{s}^{(j)}$, thus

$$\mathbf{u}_{k+1}^{(j)} \leftarrow \text{prox}_{g_j/\mu_j}(\mathbf{s}^{(j)}) \equiv \arg \min_{\mathbf{x}} \frac{1}{2} \|\mathbf{x} - \mathbf{s}^{(j)}\|_2^2 + \frac{g_j(\mathbf{x})}{\mu_j}.$$

For some functions, the Moreau proximity operators are known in closed form [9]; a well-known case is the ℓ_1 norm ($\gamma \|\mathbf{x}\|_1 = \gamma \sum_i |x_i|$), for which the proximity operator is the component-wise application of the soft threshold function: $\text{soft}(v, \gamma) = \text{sign}(v) \max\{|v| - \gamma, 0\}$.

The resulting ADMM for problem (2) is presented in Algorithm 2. The convergence conditions given in *Theorem 1* for the standard ADMM translate, in the present formulation, to the following: (i) for g to be a proper, closed, convex function, it suffices that each function g_j be itself proper, closed, and convex; (ii) for matrix \mathbf{G} , as given in (3), to be of full-column rank, a sufficient condition is that one the matrices $\mathbf{H}^{(j)}$ has full column rank. If \mathbf{G} has full column rank, a sufficient condition for the inverse in (6) to exist is that $\mu_j > 0$, for $j = 1, \dots, J$.

If the proximity operators of the functions g_j are computationally inexpensive, the computational bottleneck of Algorithm 2 is the matrix inversion in line 6. As shown in [23] and [24], these matrix inversions can be efficiently tackled

Algorithm 2: ADMM-2

```

1 Initialization: set  $k = 0$ , choose  $\mu_1, \dots, \mu_J > 0$ ,  $\mathbf{u}_0, \mathbf{d}_0$ .
2 repeat
3    $\boldsymbol{\zeta} \leftarrow \mathbf{u}_k + \mathbf{d}_k$ 
4    $\mathbf{z}_{k+1} \leftarrow \left[ \sum_{j=1}^J \mu_j (\mathbf{H}^{(j)})^T \mathbf{H}^{(j)} \right]^{-1} \left( \sum_{j=1}^J \mu_j (\mathbf{H}^{(j)})^T \boldsymbol{\zeta}^{(j)} \right)$ 
5   for  $j = 1$  to  $J$  do
6      $\mathbf{u}_{k+1}^{(j)} \leftarrow \text{prox}_{g_j/\mu_j}(\mathbf{H}^{(j)} \mathbf{z}_{k+1} - \mathbf{d}_k^{(j)})$ 
7      $\mathbf{d}_{k+1}^{(j)} \leftarrow \mathbf{d}_k^{(j)} - (\mathbf{H}^{(j)} \mathbf{z}_{k+1} - \mathbf{u}_{k+1}^{(j)})$ 
8   end
9    $k \leftarrow k + 1$ 
10 until stopping criterion is satisfied

```

using the FFT, if all the matrices $\mathbf{H}^{(j)}$ are circulant, thus diagonalized by the DFT¹ (more details will be given in the next section). Because of this condition, the work in [23] and [24] was limited to deconvolution with periodic boundary conditions, under TV regularization. More recent work in [2], [3], [14] has shown how this inversion can still be efficiently handled using the FFT (and other fast transforms) in other problems, such as image reconstruction from partial Fourier observations and inpainting, and with other regularizers, such as those based on tight frames. In the next section, we will show how to handle deconvolution problems with unknown boundary conditions.

III. PROPOSED APPROACH

This section presents the proposed approach for image deconvolution with unknown boundary conditions. The approach will be described in the context of image deconvolution under TV regularization [20], [23], as this is, arguably, the most standard regularizer for this class of imaging inverse problems. Extension to other regularizers, namely frame-based analysis or synthesis formulations [2], [3], [14], is straightforward. Before addressing the non-cyclic deblurring case, we review the cyclic deblurring case, which will provide the basic elements and structure for the proposed method.

A. TV-Based Deconvolution with Periodic Boundary Conditions

The classical formulation of TV-based image deconvolution consists of a convex optimization problem

$$\hat{\mathbf{x}} = \arg \min_{\mathbf{x} \in \mathbb{R}^n} \frac{1}{2} \|\mathbf{y} - \mathbf{A}\mathbf{x}\|_2^2 + \lambda \sum_{i=1}^n \|\mathbf{D}_i \mathbf{x}\|_2, \quad (8)$$

¹In fact, since we are dealing with two-dimensional (2D) images, these matrices need to be block-circulant with circulant blocks (BCCB) to be diagonalized by the 2D DFT. For simplicity, we refer to BCCB matrices simply as circulant and to the 2D DFT simply as DFT.

where: $\mathbf{x}, \mathbf{y} \in \mathbb{R}^n$ are vectors containing all the pixels (in lexicographic order) of the sharp and degraded images, respectively; $\mathbf{A} \in \mathbb{R}^{n \times n}$ is a matrix representation of the convolution (under periodic boundary conditions) with some kernel; $\mathbf{D}_i \in \mathbb{R}^{2 \times n}$ is the matrix that computes the horizontal and vertical differences at pixel i (also with periodic boundary conditions) [23], [24]; $\lambda \geq 0$ is the regularization parameter. The sum $\sum_{i=1}^n \|\mathbf{D}_i \mathbf{x}\|_2 = \text{TV}(\mathbf{x})$ defines the so-called *total-variation*² (TV) of image \mathbf{x} . The first term in (8) results from assuming that \mathbf{y} is a noisy version of the convolved image $\mathbf{A}\mathbf{x}$, where the noise is white and Gaussian with unit variance (assuming unit variance implies no loss of generality, since any other value may be absorbed by the regularization parameter λ).

Clearly, problem (8) has the form (2), with the following mapping: $J = n + 1$,

$$g_i : \mathbb{R}^2 \rightarrow \mathbb{R}, \quad g_i(\mathbf{v}) = \lambda \|\mathbf{v}\|_2, \quad \text{for } i = 1, \dots, n, \quad (9)$$

$$g_{n+1} : \mathbb{R}^n \rightarrow \mathbb{R}, \quad g_{n+1}(\mathbf{v}) = \frac{1}{2} \|\mathbf{y} - \mathbf{v}\|_2^2, \quad (10)$$

$$\mathbf{H}^{(i)} = \mathbf{D}_i \in \mathbb{R}^{2 \times n}, \quad \text{for } i = 1, \dots, n, \quad (11)$$

$$\mathbf{H}^{(n+1)} = \mathbf{A} \in \mathbb{R}^{n \times n}. \quad (12)$$

Concerning matrix $\boldsymbol{\Upsilon}$ (see (5)), we adopt $\mu_j = \alpha > 0$, for $j = 1, \dots, n$, and $\mu_{n+1} = \beta > 0$. With these choices, and the mapping in (9)–(12), the fundamental steps of Algorithm 2 are as follows.

- As shown in [23], [24], the matrix to be inverted in line 4 of Algorithm 2 can be written as

$$\alpha \sum_{j=1}^n \mathbf{D}_j^T \mathbf{D}_j + \beta \mathbf{A}^T \mathbf{A} = \alpha (\mathbf{D}^h)^T \mathbf{D}^h + \alpha (\mathbf{D}^v)^T \mathbf{D}^v + \beta \mathbf{A}^T \mathbf{A}, \quad (13)$$

where $\mathbf{D}^h \in \mathbb{R}^{n \times n}$ (respectively, $\mathbf{D}^v \in \mathbb{R}^{n \times n}$) is the matrix collecting the first row of each of the n matrices \mathbf{D}_i (respectively, the second row of each of the n matrices \mathbf{D}_i); that is, \mathbf{D}^h computes all the horizontal differences and \mathbf{D}^v all the vertical differences. Assuming periodic boundary conditions, all the matrices in (13) are circulant, thus can be factorized as $\mathbf{A} = \mathbf{U}^T \boldsymbol{\Lambda} \mathbf{U}$, $\mathbf{D}^h = \mathbf{U}^T \boldsymbol{\Delta}^h \mathbf{U}$, and $\mathbf{D}^v = \mathbf{U}^T \boldsymbol{\Delta}^v \mathbf{U}$, where \mathbf{U} is the unitary matrix ($\mathbf{U}^{-1} = \mathbf{U}^T$) corresponding to the DFT, while $\boldsymbol{\Lambda}$, $\boldsymbol{\Delta}^h$, and $\boldsymbol{\Delta}^v$ are diagonal matrices. Consequently, the inverse of the matrix in (13) can be written as

$$\left(\alpha (\mathbf{D}^h)^T \mathbf{D}^h + \alpha (\mathbf{D}^v)^T \mathbf{D}^v + \beta \mathbf{A}^T \mathbf{A} \right)^{-1} = \mathbf{U}^T (\alpha |\boldsymbol{\Delta}^h|^2 + \alpha |\boldsymbol{\Delta}^v|^2 + \beta |\boldsymbol{\Lambda}|^2)^{-1} \mathbf{U}, \quad (14)$$

which involves a diagonal inversion (with $O(n)$ cost) and the products by \mathbf{U} and \mathbf{U}^T (the direct and inverse discrete Fourier transforms), which have $O(n \log n)$ cost, if implemented by the FFT.

- The sum defining the vector to which this inverse is ap-

²In fact, this is the so-called isotropic discrete approximation of the continuous total-variation norm [7], [20].

plied (line 4 of Algorithm 2) can be expressed compactly as follows:

$$\begin{aligned} \sum_{j=1}^J \mu_j (\mathbf{H}^{(j)})^T \boldsymbol{\zeta}^{(j)} &= \alpha \sum_{j=1}^n \mathbf{D}_j^T \boldsymbol{\zeta}^{(j)} + \beta \mathbf{A}^T \boldsymbol{\zeta}^{(n+1)} \\ &= \beta \mathbf{A}^T \boldsymbol{\zeta}^{(n+1)} + \alpha (\mathbf{D}^h)^T \boldsymbol{\delta}^h + \alpha (\mathbf{D}^v)^T \boldsymbol{\delta}^v, \end{aligned}$$

where $\boldsymbol{\delta}^h \in \mathbb{R}^n$ (respectively, $\boldsymbol{\delta}^v \in \mathbb{R}^n$) contains the first (respectively, the second) component of all the $\boldsymbol{\zeta}^{(j)}$ vectors, for $j = 1, \dots, n$. Notice that the products by matrices \mathbf{A}^T , $(\mathbf{D}^h)^T$, and $(\mathbf{D}^v)^T$ are also implemented with $O(n \log n)$ cost via the FFT (instead of the standard $O(n^2)$ cost of matrix-vector multiplications). For example, $\mathbf{A}^T \mathbf{v} = \mathbf{U}^T \boldsymbol{\Lambda} \mathbf{U} \mathbf{v}$, where the products by \mathbf{U} and \mathbf{U}^T are implemented by the FFT and $\boldsymbol{\Lambda}$ is diagonal.

- The proximity operator of $g_i(\mathbf{v}) = \lambda \|\mathbf{v}\|_2$, for $i = 1, \dots, n$, is given by the so-called vector-soft function [23], [24], which is the generalization of the soft thresholding function for vector arguments:

$$\begin{aligned} \text{prox}_{\lambda \|\cdot\|_2}(\mathbf{v}) &= \text{vect-soft}(\mathbf{v}, \lambda) \\ &\equiv \frac{\mathbf{v}}{\|\mathbf{v}\|_2} \max\{\|\mathbf{v}\|_2 - \lambda, 0\}, \end{aligned}$$

with the convention that $\mathbf{0}/\|\mathbf{0}\|_2 = 0$.

- The proximity operator of $g_{n+1}(\mathbf{v}) = \frac{1}{2} \|\mathbf{v} - \mathbf{y}\|_2^2$ is an affine function,

$$\text{prox}_{(\gamma/2)\|\cdot\| - \mathbf{y}\|_2^2}(\mathbf{v}) = \frac{\gamma \mathbf{y} + \mathbf{v}}{\gamma + 1}. \quad (15)$$

Plugging these equalities into Algorithm 2, we obtain Algorithm 3, which is very similar to the algorithm presented in [23]. Of course, the FFT-based implementation in line 6 is only valid under the assumption that \mathbf{A} is a circulant matrix, that is that the convolution that it represents uses periodic boundary conditions, the same being true for the difference operators represented by the \mathbf{D}_j matrices.

Finally, notice that, in general, none of the \mathbf{D}_j matrices has full column rank, and we also cannot guarantee that \mathbf{A} has full column rank. However, if \mathbf{A} corresponds to a low-pass filter with non-zero gain for constant images, matrix $\mathbf{G} = [(\mathbf{D}_1)^T, \dots, (\mathbf{D}_n)^T, \mathbf{A}^T]^T$ has full-column rank, and the conditions of *Theorem 1* are satisfied, thus guaranteeing convergence of the ADMM algorithm.

B. TV-Based Deconvolution with Unknown Boundary Conditions

To handle images with unknown boundary conditions, the observation model should express the fact that the boundary pixels are not observed; that is,

$$\mathbf{y} = \mathbf{M} \mathbf{A} \mathbf{x} + \mathbf{n}, \quad (16)$$

where \mathbf{n} denotes white Gaussian noise of unit variance and (as above) $\mathbf{A} \in \mathbb{R}^{n \times n}$ is a matrix representation of the convolution with some kernel; the new element in (16) is $\mathbf{M} \in \mathbb{R}^{m \times n}$ (with $m < n$), which is a masking matrix, *i.e.*, a matrix whose rows are a subset of the rows of an identity matrix. The role of the masking matrix is to observe only the subset of the

Algorithm 3: ADMM-TV

```

1 Set  $k = 0$ , choose  $\alpha, \beta > 0$ ,  $\mathbf{u}_0^{(j)}$  and  $\mathbf{d}_0^{(j)}$ , for
    $j = 1, \dots, n + 1$ 
2 repeat
3    $\boldsymbol{\zeta} \leftarrow \mathbf{u}_k + \mathbf{d}_k$ 
4    $\boldsymbol{\delta}^h = [(\boldsymbol{\zeta}^{(1)})_1, \dots, (\boldsymbol{\zeta}^{(n)})_1]^T$ 
5    $\boldsymbol{\delta}^v = [(\boldsymbol{\zeta}^{(1)})_2, \dots, (\boldsymbol{\zeta}^{(n)})_2]^T$ 
6    $\mathbf{z}_{k+1} \leftarrow \mathbf{U}^T (\alpha |\boldsymbol{\Delta}^h|^2 + \alpha |\boldsymbol{\Delta}^v|^2 +$ 
       $\beta |\boldsymbol{\Lambda}|^2)^{-1} \mathbf{U} (\beta \mathbf{A}^T \boldsymbol{\zeta}^{(n+1)} + \alpha (\mathbf{D}^h)^T \boldsymbol{\delta}^h + \alpha (\mathbf{D}^v)^T \boldsymbol{\delta}^v)$ 
7   for  $j = 1$  to  $n$  do
8      $\mathbf{u}_{k+1}^{(j)} \leftarrow \text{vect-soft}(\mathbf{D}_j \mathbf{z}_{k+1} - \mathbf{d}_k^{(j)}, \frac{\lambda}{\alpha})$ 
9      $\mathbf{d}_{k+1}^{(j)} \leftarrow \mathbf{d}_k^{(j)} - (\mathbf{D}_j \mathbf{z}_{k+1} - \mathbf{u}_{k+1}^{(j)})$ 
10  end
11   $\mathbf{u}_{k+1}^{(n+1)} \leftarrow \frac{1}{1+\beta} (\mathbf{y} + \beta (\mathbf{A} \mathbf{z}_{k+1} - \mathbf{d}_k^{(n+1)}))$ 
12   $\mathbf{d}_{k+1}^{(n+1)} \leftarrow \mathbf{d}_k^{(n+1)} - (\mathbf{A} \mathbf{z}_{k+1} - \mathbf{u}_{k+1}^{(n+1)})$ 
13   $k \leftarrow k + 1$ 
14 until stopping criterion is satisfied
```

image domain in which the pixel values of $\mathbf{A} \mathbf{x}$ do not depend on the boundary pixels; consequently, the type of boundary condition assumed for the convolution represented by \mathbf{A} is irrelevant, and we may adopt periodic boundary conditions for computational convenience.

Assuming that \mathbf{A} models the convolution with a blurring filter with a limited support of size $(1+2l) \times (1+2l)$, and that $\mathbf{x} \in \mathbb{R}^n$ and $\mathbf{A} \mathbf{x} \in \mathbb{R}^n$ represent square images of dimensions $\sqrt{n} \times \sqrt{n}$, then matrix $\mathbf{M} \in \mathbb{R}^{m \times n}$, with $m = (\sqrt{n} - 2l)^2$, represents the removal of a band of width l of the outermost pixels of the full convolved image $\mathbf{A} \mathbf{x}$.

Under the model in (16), TV-based deconvolution with unknown boundary conditions is formulated as

$$\hat{\mathbf{x}} = \arg \min_{\mathbf{x} \in \mathbb{R}^n} \frac{1}{2} \|\mathbf{y} - \mathbf{M} \mathbf{A} \mathbf{x}\|_2^2 + \lambda \sum_{i=1}^n \|\mathbf{D}_i \mathbf{x}\|_2, \quad (17)$$

where λ and the matrices \mathbf{D}_i have exactly the same meaning as in (8). Problem (17) can be seen as hybrid of deconvolution and inpainting, where the missing pixels constitute the unknown boundary. If matrix \mathbf{M} is assumed to be the identity, problem (17) reduces to TV-regularized periodic deconvolution (as in (8)). Conversely, (17) becomes a pure inpainting problem if \mathbf{A} is identity. Moreover, the formulation (17) can be applied to problems where not only the boundary, but also other pixels, are missing (for example, due to saturation of the image sensor).

At this point, one could be tempted to map (17) into (2) using the same mappings as in (9)–(12), with $\mathbf{M}\mathbf{A}$ replacing \mathbf{A} in (12). However, unlike \mathbf{A} , matrix $\mathbf{M}\mathbf{A}$ is not circulant (it is not even square), thus it is not diagonalized by the DFT, and the inversion in line 4 of Algorithm 3 cannot be computed efficiently as in (14). To sidestep this difficulty, we propose to replace the mapping (10) by

$$g_{n+1}(\mathbf{v}) = \frac{1}{2} \|\mathbf{y} - \mathbf{M}\mathbf{v}\|_2^2, \quad (18)$$

and leave the mapping (12) unchanged. The only resulting change to Algorithm 3 is in line 11, because g_{n+1} is no longer given as in (10), but is now as defined in (18). The proximity operator of $g_{n+1}(\mathbf{v}) = \frac{1}{2} \|\mathbf{M}\mathbf{v} - \mathbf{y}\|_2^2$ is given by

$$\begin{aligned} \text{prox}_{(\gamma/2)\|\mathbf{M}\cdot - \mathbf{y}\|_2^2}(\mathbf{v}) &= \arg \min_{\mathbf{u}} \gamma \|\mathbf{M}\mathbf{u} - \mathbf{y}\|_2^2 + \|\mathbf{u} - \mathbf{v}\|_2^2 \\ &= (\gamma \mathbf{M}^T \mathbf{M} + \mathbf{I})^{-1} (\gamma \mathbf{M}^T \mathbf{y} + \mathbf{v}). \end{aligned} \quad (19)$$

Notice that (15) is a special case of (19) for $\mathbf{M} = \mathbf{I}$. Due to the structure of \mathbf{M} (its rows are a subset of the rows of an identity), matrix $\mathbf{M}^T \mathbf{M}$ is diagonal and so is $\gamma \mathbf{M}^T \mathbf{M} + \mathbf{I}$, its inversion thus being trivial and having $O(n)$ cost. Observe also that $\mathbf{M}^T \mathbf{y}$ is the extension of the observed image to the same size as \mathbf{x} , by creating a boundary of zeros around it.

In summary, the algorithm herein proposed for TV-based deconvolution with unknown boundary conditions has the exact same structure as Algorithm 3, with line 11 replaced by the following expression:

$$\mathbf{u}_{k+1}^{(n+1)} \leftarrow (\mathbf{M}^T \mathbf{M} + \beta \mathbf{I})^{-1} (\mathbf{M}^T \mathbf{y} + \beta (\mathbf{A} \mathbf{z}_{k+1} - \mathbf{d}_k^{(n+1)}));$$

notice that since $(\mathbf{M}^T \mathbf{M} + \beta \mathbf{I})^{-1}$ is a diagonal matrix, multiplying by it is equivalent to element-wise multiplication by a vector. The cost per iteration of the algorithm is dominated by the $O(n \log n)$ of the FFT implementations of the products by the DFT matrices \mathbf{U} and \mathbf{U}^T (line 6).

IV. EXPERIMENTS

A. Deblurring with unknown boundary conditions

The proposed ADMM approach for image deconvolution with unknown boundary conditions was tested on the benchmark images “Lena” and “cameraman”, degraded with 4 different blurring filters (out-of-focus, linear motion, uniform, and Gaussian), all of size 9×9 (i.e., $(2l+1) \times (2l+1)$, with $l=4$), at three different noise levels: 40 dB, 35 dB, and 30 dB of *blurred signal to noise ratio* (BSNR). The images are blurred using non-cyclic convolution, where the external region (of width $l=4$) is obtained by copying the boundary rows and columns 4 times; that is, the external region above the image contains 4 copies of the first row, and similarly for the other boundaries. Of course, the deconvolution algorithm does not have this information.

Different ADMM approaches for TV-regularized deconvolution were considered: (1) ignoring the non-periodic nature of the convolution, i.e., assuming (wrongly) that the convolution is periodic (this approach will be referred to as “old”); (2) using the approach proposed in Subsection III-B of this paper (which will be referred to as “new”); (3) preprocessing

the blurred images using the “edgetaper” Matlab function, but ignoring the non-periodic nature of the convolution (this approach will be referred to as “tapered”); (4) using the strategy described in the appendix, which will be referred to as “CG”.

The regularization parameter λ was manually adjusted to yield the best ISNR (*improvement in signal to noise ratio*) for each experimental condition. For the ADMM parameters (α and β), which affect the convergence speed, we used heuristic rules, which lead to a good performance of the algorithm: β was chosen to be proportional to λ specifically $\beta = 10\lambda$; concerning α , we used the heuristic rule $\alpha = \min\{1, 5000\beta\}$.

Tables I and II show the average ISNR values and the processing complexities and times of the algorithms considered. The processing time is presented in seconds³ and the complexity measured by the number of calls to the FFT algorithm required per iteration. The inability of the baseline method (“old”) to address non-cyclic deconvolution is evident from Table I, while the approaches that model the boundary as unknown are clearly better. In terms of ISNR, the new method proposed in Subsection III-B and the one described in the appendix yield essentially identical values, which is a natural and reassuring fact, since both methods attack the same optimization problem. However, our approach (“new”) is considerably faster than “CG”, having approximately half of the complexity per iteration of the method described in the appendix. In addition to being faster than “CG”, our approach is also considerably simpler to implement, since it does not involve any inner iterative solver. To serve as benchmark, Tables I and II also show results for the baseline method (“old”) for observed images obtained with periodic convolutions. The visual advantage of the proposed approach over the “old” and the “tapered” methods are illustrated in Figures 2 and 3. The boundary ripple artifacts resulting from an incorrect convolution model are quite evident in “old” approach and still visible in the “tapered” method. In contrast, these boundary artifacts are essentially absent with the “new” approach, whose results are visually similar to the (ideal) ones obtained for cyclic degradations. The restored images obtained with the “CG” method are visually indistinguishable from those obtained with the new method, so we don’t show them.

B. Simultaneous deconvolution and inpainting

The proposed method was also successfully tested in simultaneous non-cyclic deblurring and inpainting. As an example of the performance of our method, Figure 4 shows the results obtained for the “cameraman” image, non-periodically blurred with a 9×9 uniform blur (assuming the same boundary conditions explained in the previous experiments), with 40dB BSNR, and with 20% of missing pixels.

V. CONCLUSIONS

We presented a new strategy to extend recent fast algorithms for image deconvolution, based on the *alternating direction method of multipliers* (ADMM), to problems with unknown

³The methods were implemented in Matlab and run on a Intel Core i5 processor at 2.39GHz.

	Non-cyclic				Cyclic
	old	tapered	CG	new	old
40dB Lena	-1.63	6.34	7.50	7.49	7.91
40dB Cameraman	1.23	7.51	8.52	8.53	8.81
35dB Lena	1.24	6.52	6.99	6.99	7.19
35dB Cameraman	-1.62	5.70	6.16	6.15	6.53
30dB Lena	-1.63	4.91	5.01	5.00	5.34
30dB Cameraman	1.25	5.42	5.62	5.62	5.76

TABLE I

COMPARISON OF DIFFERENT APPROACHES; THE ISNR VALUES ARE COMPUTED FOR THE VALID PIXELS AND AVERAGED OVER THE TWO IMAGES AND THE FOUR BLURRING FILTERS CONSIDERED.

	Non-cyclic				Cyclic
	old	tapered	CG	new	old
FFT/iter.	7	7	13	7	7
time/iter.	0.030	0.031	0.069	0.035	0.031

TABLE II

COMPUTATIONAL COST OF DIFFERENT APPROACHES, MEASURED IN NUMBER OF FFTS AND PROCESSING TIME (SECONDS) PER ITERATION.

boundary conditions. The proposed approach is also able to address a more general class of problems where the degradation model consists of a combination of a convolution (blurring) and a loss of pixels. Our approach is validated by adapting a recent state-of-the-art algorithm for deconvolution under total variation regularization [23], and comparing it with the recent approach of [21]. The proposed technique was shown to attain results similar to those obtained with the technique of [21], while being simpler and requiring roughly half of the processing time.

APPENDIX: TV-BASED DECONVOLUTION WITH UNKNOWN BOUNDARY CONDITIONS USING THE REEVES-SOREL APPROACH

A key feature of the approach proposed in Subsection III-B is that each step of the ADMM algorithm is computed in closed form, without the need for any inner iterations. In this appendix, we describe an alternative approach (which does not share this desirable property) based on a technique proposed in [19], and that was also very recently used in [21]. The goal of this appendix is to adapt the method proposed in [21] to the ADMM formulation and notation used in this paper. Let the objective function in (17) be mapped into the form (2) as in (9)–(12), with \mathbf{MA} replacing \mathbf{A} in (12). As mentioned in Subsection III-B, matrix \mathbf{MA} is not circulant, thus it is not diagonalized by the DFT, and the inversion in line 4 of Algorithm 3 cannot be computed efficiently as in (14). Following [21], that inversion can be addressed using the technique introduced in [19].



Fig. 2. Deblurring results obtained for the “Lena” image blurred with the uniform filter, at 40dB BSNR. From left to right: “old” ($ISNR = -2.67dBs$), “tapered” ($ISNR = 5.52dBs$), “new” ($ISNR = 7.09dBs$) and “ideal” (cyclic degradation, $ISNR = 7.52dBs$).

With \mathbf{MA} replacing \mathbf{A} , the matrix to be inverted in each iteration of ADMM is given by

$$\alpha(\mathbf{D}^h)^T \mathbf{D}^h + \alpha(\mathbf{D}^v)^T \mathbf{D}^v + \beta \mathbf{A}^T \mathbf{M}^T \mathbf{MA}; \quad (20)$$

although \mathbf{D}^h , \mathbf{D}^v , and \mathbf{A} are circulant, this matrix cannot be inverted as in (14), due to the presence of \mathbf{M} . As in [19], let

$$\mathbf{A} = \mathbf{P} \begin{bmatrix} \mathbf{MA} \\ \mathbf{b} \end{bmatrix}$$

where \mathbf{b} contains the rows of \mathbf{A} that are missing from \mathbf{MA} and \mathbf{P} is a permutation matrix that puts these missing rows in their original positions in \mathbf{A} . To simplify the notation, write $\mathbf{V} = \alpha(\mathbf{D}^h)^T \mathbf{D}^h + \alpha(\mathbf{D}^v)^T \mathbf{D}^v$. Noticing that

$$\mathbf{A}^T \mathbf{A} = [\mathbf{A}^T \mathbf{M}^T, \mathbf{b}^T] \mathbf{P}^T \mathbf{P} \begin{bmatrix} \mathbf{MA} \\ \mathbf{b} \end{bmatrix} = \mathbf{A}^T \mathbf{M}^T \mathbf{MA} + \mathbf{b}^T \mathbf{b}$$

(because \mathbf{P} is a permutation matrix, thus orthogonal), the matrix inversion can be written as

$$(\mathbf{V} + \beta \mathbf{A}^T \mathbf{M}^T \mathbf{MA})^{-1} = (\mathbf{V} + \beta \mathbf{A}^T \mathbf{A} - \beta \mathbf{b}^T \mathbf{b})^{-1} \\ = \mathbf{C} - \mathbf{C} \mathbf{b}^T (\mathbf{b} \mathbf{C} \mathbf{b}^T - (1/\beta) \mathbf{I})^{-1} \mathbf{b} \mathbf{C}, \quad (21)$$

where the second equality results from setting $\mathbf{C} = (\mathbf{V} + \beta \mathbf{A}^T \mathbf{A})^{-1}$ and using the Sherman-Morrison-Woodbury matrix inversion identity. The inversion $\mathbf{C} = (\mathbf{V} + \beta \mathbf{A}^T \mathbf{A})^{-1} = (\alpha(\mathbf{D}^h)^T \mathbf{D}^h + \alpha(\mathbf{D}^v)^T \mathbf{D}^v + \beta \mathbf{A}^T \mathbf{A})^{-1}$ can be efficiently computed via FFT, as in (14). The inner inversion in (21) cannot be computed via FFT; however, its dimension corresponds to the number of unknown boundary pixels (number of rows in \mathbf{b}), thus it is usually much smaller than \mathbf{x} . As in [19], [21],

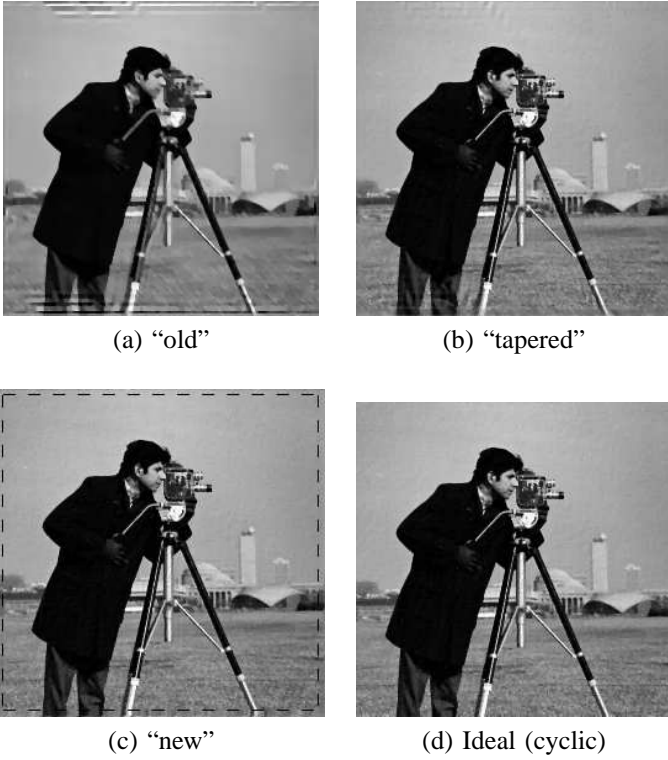


Fig. 3. Deblurring results obtained for the "cameraman" image blurred with the linear motion filter, at 40dB BSNR. From left to right: "old" ($ISNR = 2.03dBs$), "tapered" ($ISNR = 9.07dBs$), "new" ($ISNR = 10.08dBs$), and "ideal" (cyclic degradation, $ISNR = 10.47dBs$).

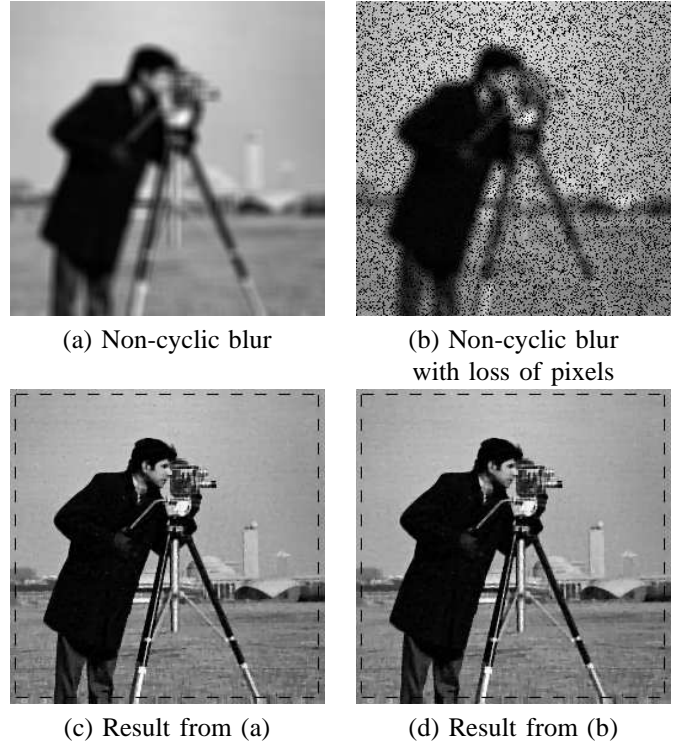


Fig. 4. Results obtained, with our approach, for the cameraman image degraded with a non-cyclic convolution with a 9×9 uniform blur, at 40dB BSNR, followed by loss of 20% of the pixels: (a) blurred image, (b) blurred image with 20% missing pixels, (c) and (d) images recovered from (a) and (b), respectively.

we adopt the conjugate-gradient (CG) algorithm to solve the corresponding system; we verified experimentally that taking only one CG iteration in each ADMM iteration yields the best results and is the fastest option.

REFERENCES

- [1] M. V. Afonso, J. M. Bioucas-Dias, and M. A. T. Figueiredo, "An augmented Lagrangian approach to linear inverse problems with compound regularization," in *IEEE Intern. Conf. on Image Processing – ICIP*, 2010.
- [2] —, "Fast image recovery using variable splitting and constrained optimization," *IEEE Trans. on Image Processing*, vol. 19, pp. 2345–2356, 2010.
- [3] —, "An augmented lagrangian approach to the constrained optimization formulation of imaging inverse problems," *IEEE Transactions on Image Processing*, vol. 20, pp. 681–695, 2011.
- [4] —, "Non-cyclic deconvolution using an augmented lagrangian method," in *IEEE International Conference on Computer as a Tool (EUROCON)*, 2011, pp. 1–4.
- [5] S. Boyd, N. Parikh, E. Chu, B. Peleato, and J. Eckstein, "Distributed optimization and statistical learning via the alternating direction method of multipliers," *Foundations and Trends in Machine Learning*, vol. 3, no. 1, pp. 1–122, 2011.
- [6] J.-F. Cai, S. Osher, and Z. Shen, "Split Bregman methods and frame based image restoration," *Multiscale Model. Simul.*, vol. 8, no. 2, pp. 337–369, 2009.
- [7] A. Chambolle, "An algorithm for total variation minimization and applications," *Journal of Mathematical Imaging and Vision*, vol. 20, pp. 89–97, 2004.
- [8] T. F. Chan, A. M. Yip, and F. E. Park, "Simultaneous total variation image inpainting and blind deconvolution," *International Journal of Imaging Systems and Technology*, vol. 15, no. 1, pp. 92–102, 2005.
- [9] P. L. Combettes and J.-C. Pesquet, "A Douglas-Rachford splitting approach to nonsmooth convex variational signal recovery," *IEEE Journal of Selected Topics in Signal Processing*, vol. 1, pp. 564–574, 2007.
- [10] P. L. Combettes and V. Wajs, "Signal recovery by proximal forward-backward splitting," *SIAM Journal on Multiscale Modeling & Simulation*, vol. 4, pp. 1168–1200, 2005.
- [11] M. Donatelli, C. Estatico, A. Martinelli, and S. Serra-Capizzano, "Improved image deblurring with anti-reflective boundary conditions and re-blurring," *Inverse Problems*, vol. 22, no. 6, pp. 2035–2053, 2006.
- [12] J. Eckstein and D. P. Bertsekas, "On the douglas-rachford splitting method and the proximal point algorithm for maximal monotone operators," *Mathematical Programming*, vol. 55, pp. 293–318, 1992.
- [13] E. Esser, "Applications of Lagrangian based alternating direction methods and connections to split Bregman," UCLA, Tech. Rep. 09-31, 2009.
- [14] M. A. T. Figueiredo and J. M. Bioucas-Dias, "Restoration of Poissonian images using alternating direction optimization," *IEEE Trans. on Image Processing*, vol. 19, pp. 3133–314, 2010.
- [15] D. Gabay and B. Mercier, "A dual algorithm for the solution of nonlinear variational problems via infinite element approximations," *Computers and Mathematics with Applications*, vol. 2, p. 1740, 1976.
- [16] T. Goldstein and S. Osher, "The split bregman method for l1-regularized problems," *SIAM J. Img. Sci.*, vol. 2, pp. 323–343, April 2009.
- [17] R. Liu and J. Jia, "Reducing boundary artifacts in image deconvolution," in *IEEE Intern. Conf. on Image Processing – ICIP*, 2008, pp. 505–508.
- [18] S. Ramani and J. Fessler, "A splitting-based iterative algorithm for accelerated statistical X-ray CT reconstruction," *IEEE Trans. on Medical Imaging*, vol. 31, pp. 677–688, 2012.
- [19] S. J. Reeves, "Fast image restoration without boundary artifacts," *IEEE Trans. on Image Processing*, vol. 14, no. 10, pp. 1448–1453, 2005.
- [20] L. Rudin, S. Osher, and E. Fatemi, "Nonlinear total variation based noise removal algorithms," *Physica-D*, vol. 60, pp. 259–268, 1992.
- [21] M. Sorel, "Removing boundary artifacts for real-time iterated shrinkage deconvolution," *IEEE Trans. on Image Processing*, vol. 21, no. 4, pp. 2329–2334, 2012.
- [22] G. Steidl and T. Teuber, "Removing multiplicative noise by Douglas-Rachford splitting methods," *Journal of Mathematical Imaging and Vision*, vol. 36, no. 2, pp. 168–184, 2010.
- [23] M. Tao and J. Yang, "Alternating direction algorithms for total variation deconvolution in image reconstruction," Department of Mathematics, Nanjing University, Tech. Rep. TR0918, 2009, (available at http://www.optimization-online.org/DB_HTML/2009/11/2463.html).
- [24] Y. Wang, J. Yang, W. Yin, and Y. Zhang, "A new alternating minimization algorithm for total variation image reconstruction," *SIAM J. Imaging Sci.*, vol. 1, no. 3, pp. 248–272, 2008.

- [25] W. Yin, S. Osher, D. Goldfarb, and J. Darbon, “Bregman iterative algorithms for ℓ_1 -minimization with applications to compressed sensing,” *SIAM Journal on Imaging Sciences*, vol. 1, no. 1, pp. 143–168, 2008.
- [26] L. Zappella, A. Del Bue, X. Llado, and J. Salvi, “Simultaneous motion segmentation and structure from motion,” in *IEEE Workshop on Applications of Computer Vision (WACV)*, 2011, pp. 679–684.